J. Biochem. **144,** 63–76 (2008)
doi:10.1093/jb/mvn044

Identification of the Coiled-coil Domains of *Enterococcus faecalis* DivIVA that Mediate Oligomerization and their Importance for Biological Function

Marc D. Rigden[1], Cherise Baier[2], Sandra Ramirez-Arcos[1,*], Mingmin Liao[2,3], Monica Wang[3,4] and Jo-Anne R. Dillon[1,2,3,4,†,‡]

[1]Department of Biochemistry, Microbiology and Immunology, University of Ottawa, 451 Smyth Road, Ottawa, Ontario K1H 8M5; [2]Department of Microbiology and Immunology, 107 Wiggins Road, Saskatoon, Saskatchewan S7N 5E5; [3]Vaccine and Infectious Disease Organization, 120 Veterinary Road, Saskatoon, Saskatchewan S7N 5E3; and [4]Department of Biology, University of Saskatchewan, 112 Science Place, Saskatoon, Saskatchewan, S7N 5E2, Canada

Received October 24, 2007; accepted March 13, 2008; published online April 3, 2008

***Bacillus subtilis* (Bs) DivIVA comprises coiled-coil structures and self-associates forming a 10–12 mer complex *in vitro*. Using bioinformatic approaches, we determined that *Enterococcus faecalis* (Ef) DivIVA comprises four coiled-coil domains, one at the N-terminus, the second and the third in the central region of the protein and the fourth at the C-terminus. We determined that $DivIVA_{Ef}$ self-interacts and forms a 10–12 multimeric complex. Point mutations or deletions of the central regions predicted bioinformatically to disrupt the coiled-coil structures either eliminated or weakened $DivIVA_{Ef}$ self-interaction and reduced oligomerization. Mutations disrupting the N- and C-terminal coiled-coils of $DivIVA_{Ef}$ did not affect $DivIVA_{Ef}$ oligomerization. The introduction of $DivIVA_{Ef}$ mutations to both the N-terminal and the central coiled-coil domains were lethal unless rescued by expressing wild-type $DivIVA_{Ef}$ *in trans*. *E. faecalis* cells expressing these mutations displayed aberrant cell morphology, indicating disruption of the normal cell division phenotype. The results in *E. faecalis* also indicate that both the N-terminal and the central coiled-coil structures of $DivIVA_{Ef}$ are indispensable for proper biological function. Overexpression of wild-type $DivIVA_{Ef}$ in both rod-shaped and round *Escherichia coli* cells resulted in morphological changes, while the overexpression of $DivIVA_{Ef}$ mutations failed to induce such alterations.**

Key words: cell division, DivIVA, *Enterococcus faecalis*, mutagenesis, protein interactions.

Abbreviations: Bs, *Bacillus subtilis*; $DivIVA_{Ef}$, *E. faecalis* DivIVA; Ef, *Enterococcus faecalis*; NGE, Native Gel Electrophoresis; SDM, site-directed mutagenesis; SEC, size exclusion chromatography; Y2H, yeast two-hybrid assays.

INTRODUCTION

DivIVA is implicated in cell division primarily in Gram positive bacteria (*1–4*), although a homologue of this protein is also present in the Gram negative microorganism *Myxococcus xanthus* (*5*). In *Bacillus subtilis* (Bs), DivIVA regulates the placement of the MinC and MinD cell division inhibitory complex by sequestering these proteins to the cell poles, allowing for FtsZ-ring formation at the mid-cell (*6–8*). DivIVA also plays a role in chromosome segregation in *B. subtilis* (*9*), *Streptococcus pneumoniae* (*10*) and *Enterococcus faecalis* (Ef) (*4*); on apical growth and morphology in *Brevibacterium lactofermentum* (*11*) and *Streptomyces coelicolor* (*12*) and, on sporulation in *B. subtilis* (*9*, *13*). *E. faecalis* (*4*) and other Gram positive cocci, such as *S. pneumoniae* (*10*, *14*, *15*) and *Staphylococcus aureus* (*16*), contain a DivIVA homologue but lack any Min proteins. In *E. faecalis*, DivIVA is essential for cell viability and is involved in cell division and chromosome segregation (*4*), similar to its counterpart in *S. pneumoniae* (*10*, *14*). However, inactivation of *divIVA* in *S. aureus* did not result in abnormal cell division (*16*). Furthermore, *E. faecalis* DivIVA failed to complement the cell division defects of either *S. pneumoniae* or *B. subtilis divIVA* mutants, reflecting the diversity of DivIVA function in various microorganisms and indicating that DivIVA may be a species-specific cell division protein (*4*).

The functional diversity of DivIVA proteins from various bacteria could be attributed to differences in their protein sequence compositions and structures (*2*, *10*, *11*, *16*). In *B. subtilis* DivIVA comprises 164 amino acids, contains a predicted N-terminal and central α-helical coiled-coil structure and forms an oligomer

*Present addresses: Canadian Blood Services, 1800 Alta Vista Drive, Ottawa, Ontario, Canada K1G 4J5.
†College of Arts and Science, University of Saskatchewan, Room 226, Arts Building, 9 Campus Drive, Saskatoon, Saskatchewan, Canada S7N 5A5.
‡To whom correspondence should be addressed. Tel: 1-306-966-4232, Fax: 1-306-966-8839, E-mail: j.dillon@usask.ca

comprising 10–12 monomers (*9*, *17–19*). The central coiled-coil structure of $DivIVA_{Bs}$ was implicated in oligomer formation (*2*, *17*) and its disruption by the introduction of proline at residue L120 (L120P) reduced the size of the oligomeric complex by 50%, as compared to wild-type $DivIVA_{Bs}$ (*17*). A *B. subtilis* strain carrying a *divIVA* L120P mutation exhibited aberrant morphologies including elongated cells, mini-cells and partially formed septa, indicating that DivIVA oligomerizaton was important for biological function (*17*). However, the interaction site for DivIVA oligomer formation was not elucidated. The potential functionality of monomeric DivIVA is unknown. In the present study, we identified the coiled-coil domains in DivIVA from *E. faecalis* ($DivIVA_{Ef}$) using bioinformatic analysis, investigated whether $DivIVA_{Ef}$ oligomerizes and whether $DivIVA_{Ef}$ oligomerization is mediated by coiled-coil domains. We created mutations in $DivIVA_{Ef}$ designed to disrupt its coiled-coil regions and then determined the effects of these mutations on the oligomerization of the protein, as well as the biological impact of such mutations when the mutated proteins were expressed in either *E. faecalis* or *E. coli*.

MATERIALS AND METHODS

Strains and Growth Conditions—Bacterial and yeast strains used in this study are described in Table 1, panel A. *Escherichia coli* XL1-Blue and DH5α were used as hosts for cloning. *Escherichia coli* C41 (DE3) (*20*) was used as a host for his-tagged $DivIVA_{Ef}$ protein expression. Rod-shaped (PB103) or round (KJB24) *E. coli* (*21*, *22*) were used as heterologous hosts for investigating the biological effects of overexpressing mutations in $DivIVA_{Ef}$. *Escherichia coli* was grown at 37°C in Luria-Bertani (LB) medium (Difco, Detroit, MI) supplemented with appropriate antibiotics [e.g. 50 μg/ml kanamycin (Kan) or 100 μg/ml ampicillin (Amp)]. *Enterococcus faecalis* JH2-2 (*23*) was the parental strain used for the construction of $divIVA_{Ef}$ mutations. *Enterococcus faecalis* JHRS1 (*4*) was used as a negative control in western blot assays, and *E. faecalis* JH2-2+R comprised JH2-2 cells transformed with pMSPSRDiv-2 (*4*). *Enterococcus faecalis* CBWT, MWMR5 and MWMR10 carried various chromosomal mutations in $divIVA_{Ef}$ (described subsequently). *Enterococcus faecalis* cells were grown at 37°C in Brain Heart Infusion (BHI) medium (Difco) and supplemented with appropriate antibiotics (*e.g.* 125 μg/ml erythromycin (Ery), Kan 50 μg/ml or both) as previously described (*4*). *Saccharomyces cerevisiae* SFY526 (Clontech, Palo Alto, CA) was used for the yeast two-hybrid (Y2H) assays. Yeast cells were grown at 30°C on either yeast extract-peptone-adenine-dextrose (YPAD) or synthetic dropout (SD) medium as described by the manufacturer (Clontech, Palo Alto, CA).

Bioinformatic Analysis of $DivIVA_{Ef}$—Sixty *divIVA* DNA sequences in 27 bacterial species had been annotated in the Institute for Genomic Research (TIGR) database (http://www.tigr.org, last accessed September 28, 2007) and the deduced amino acid sequences for these DNA sequences were retrieved from GenBank

Table 1. **Strains and plasmids.**

Strains/plasmids	Relevant genotype	Source/Reference
A. Strains		
E. coli XL1-Blue	*hsdR17 supE44 recA1 endA1 gyrA46 thi relA1 lac*/F [*proAB*$^+$ *lacI*^{q} *lac*ZDM15::Tn*10*(Tet^r)]	Stratagene
E.coli DH5α	*sup*E44Δ*lac*U169 (80*lac*ZΔM15) *hsd*R17 *rec*A1 *end*A1 *gyr*96 *thi*-1 *rel*A1	Gibco-BRL
E. coli C-41 (DE3)	F$^-$ *omp T hsdS*$_B$ (r_{B-} m_{B-}) *gal dcm* Δ(*sri-recA*) 306::tn*10* (*tet*^{R}) (DE3)	*20*
E. coli PB103	*dadR1 trpE61 trpA62 tna-5 purB*$^+$	*21*
E. coli KJB24	W3110 [*rodA (Am)*]	*22*
E. faecalis JH2-2	Derived from *E. faecalis* JH2, Rif^R, Fus^R	*23*
E. faecalis JHSR1	JH2-2 *divIVA::kan* carrying pMSPSRDiv-2 (P_{divIVA}-$divIVA_{Ef}$)	*4*
E. faecalis JH2-2+R	JH2-2 carrying pMSPSRDiv-2 (P_{divIVA}-$divIVA_{Ef}$)	This study
E. faecalis CBWT	JH2-2 *kan*^{R} cassette inserted immediately downstream $divIVA_{Ef}$	This study
E. faecalis MWMR5	JH2-2 *divIVA* mutations (E37P/N43P/L46D/L50E/L57F) carrying pMSPSRDiv-2 (P_{divIVA}-$divIVA_{Ef}$)	This study
E. faecalis MWMR10	JH2-2 *divIVA* mutations (L143P) carrying pMSPSRDiv-2 (P_{divIVA}-$divIVA_{Ef}$)	This study
S. cerevisiae SFY526	*MATa ura3-52 his3-200 ade2-101 lys2-801 trp1-901 leu2-3 112 can^r gal4-542 gal80-538 URA3::GAL1$_{UAS}$- GAL1$_{TATA}$ -lacZ*	Clontech
B. Plasmids for expressing 6xHis-tagged $DivIVA_{Ef}$ proteins in *E. coli*		
pET30a	Kan^R P_{T7}::6xHis	Novagen
pSRDiv	Kan^R P_{T7}::$divIVA_{Ef}$-6xHis	*4*
pMR1	Kan^R P_{T7}::$divIVA_{Ef}$ (L29D) -6xHis	This study
pMR2	Kan^R P_{T7}::$divIVA_{Ef}$ (E37P) - 6xHis	This study
pMR3	Kan^R P_{T7}::$divIVA_{Ef}$ (E37P/N43P/L46D) - 6xHis	This study
pMR4	Kan^R P_{T7}::$divIVA_{Ef}$ (E37P/N43P/L46D/L50D/L57F) - 6xHis	This study
pMR5	Kan^R P_{T7}::$divIVA_{Ef}$ (E37P/N43P/L46D/L50E/L57F) - 6xHis	This study
pMR6	Kan^R P_{T7}::$divIVA_{Ef}$ (Δ190–233) -6xHis	This study
pMR7	Kan^R P_{T7}::$divIVA_{Ef}$ (Δ130–190) -6xHis	This study

(continued)

Table 1. **Continued.**

Strains/plasmids	Relevant genotype	Source/Reference
pMR8	Kan^R P_{T7}::*divIVA*$_{Ef}$ (Δ60–190) -6xHis	This study
pMR9	Kan^R P_{T7}::*divIVA*$_{Ef}$ (Δ60–130) -6xHis	This study
pMR10	Kan^R P_{T7}::*divIVA*$_{Ef}$ (L143P) -6xHis	This study
pMR11	Kan^R P_{T7}::*divIVA*$_{Ef}$ (L104P) - 6xHis	This study
pMR12	Kan^R P_{T7}::*divIVA*$_{Ef}$ (L104P/L143P) - 6xHis	This study
pMR13	Kan^R P_{T7}::*divIVA*$_{Ef}$ (L104P/I115P) - 6xHis	This study
pMR14	Kan^R P_{T7}::*divIVA*$_{Ef}$ (L104P/I115P/L143P) -6xHis	This study
pMR15	Kan^R P_{T7}::*divIVA*$_{Ef}$ (L104P/I115P/I125P) -6xHis	This study
pMR16	Kan^R P_{T7}::*divIVA*$_{Ef}$ (L104P/I115P/I125P/L143P) -6xHis	This study
C. Plasmids for the yeast two-hybrid assays		
pGAD424	Amp^R P_{ADH1}[a]::*gal4*(AD)[b]	Clontech
pGBT9	Amp^R P_{ADH1}::*gal4*(BD)[c]	Clontech
pSRAD-Div	Amp^R P_{ADH1}::*gal4*(AD)-*divIVA*$_{Ef}$	*4*
pSRBD-Div	Amp^R P_{ADH1}::*gal4*(BD)-*divIVA*$_{Ef}$	*4*
pMR1-AD	Amp^R P_{ADH1}::*gal4*(AD)-*divIVA*$_{Ef}$ (L29D)	This study
pMR1-BD	Amp^R P_{ADH1}::*gal4*(BD)-*divIVA*$_{Ef}$ (L29D)	This study
pMR2-AD	Amp^R P_{ADH1}::*gal4*(AD)-*divIVA*$_{Ef}$ (E37P)	This study
pMR2-BD	Amp^R P_{ADH1}::*gal4*(BD)-*divIVA*$_{Ef}$ (E37P)	This study
pMR3-AD	Amp^R P_{ADH1}::*gal4*(AD)-*divIVA*$_{Ef}$ (E37P/N43P/L46D)	This study
pMR3-BD	Amp^R P_{ADH1}::*gal4*(BD)-*divIVA*$_{Ef}$ (E37P/N43P/L46D)	This study
pMR4-AD	Amp^R P_{ADH1}::*gal4*(AD)-*divIVA*$_{Ef}$ (E37P/N43P/L46D/L50D/L57F)	This study
pMR4-BD	Amp^R P_{ADH1}::*gal4*(BD)-*divIVA*$_{Ef}$ (E37P/N43P/L46D/L50D/L57F)	This study
pMR5-AD	Amp^R P_{ADH1}::*gal4*(AD)-*divIVA*$_{Ef}$ (E37P/N43P/L46D/L50E/L57F)	This study
pMR5-BD	Amp^R P_{ADH1}::*gal4*(BD)-*divIVA*$_{Ef}$ (E37P/N43P/L46D/L50E/L57F)	This study
pMR6-AD	Amp^R P_{ADH1}::*gal4*(AD)-*divIVA*$_{Ef}$ (Δ190–233)	This study
pMR6-BD	Amp^R P_{ADH1}::*gal4*(BD)-*divIVA*$_{Ef}$ (Δ190–233)	This study
pMR7-AD	Amp^R P_{ADH1}::*gal4*(AD)-*divIVA*$_{Ef}$ (Δ130–190)	This study
pMR7-BD	Amp^R P_{ADH1}::*gal4*(BD)-*divIVA*$_{Ef}$ (Δ130–190)	This study
pMR8-AD	Amp^R P_{ADH1}::*gal4*(AD)-*divIVA*$_{Ef}$ (Δ60–190)	This study
pMR8-BD	Amp^R P_{ADH1}::*gal4*(BD)-*divIVA*$_{Ef}$ (Δ60–190)	This study
pMR9-AD	Amp^R P_{ADH1}::*gal4*(AD)-*divIVA*$_{Ef}$ (Δ60–130)	This study
pMR9-BD	Amp^R P_{ADH1}::*gal4*(BD)-*divIVA*$_{Ef}$ (Δ60–130)	This study
pMR10-AD	Amp^R P_{ADH1}::*gal4*(AD)-*divIVA*$_{Ef}$ (L143P)	This study
pMR10-BD	Amp^R P_{ADH1}::*gal4*(BD)-*divIVA*$_{Ef}$ (L143P)	This study
pMR12-AD	Amp^R P_{ADH1}::*gal4*(AD)-*divIVA*$_{Ef}$ (L104P/L143P)	This study
pMR12-BD	Amp^R P_{ADH1}::*gal4*(BD)-*divIVA*$_{Ef}$ (L104P/L143P)	This study
pMR15-AD	Amp^R P_{ADH1}::*gal4*(AD)-*divIVA*$_{Ef}$ (L104P/I115P/I125P)	This study
pMR15-BD	Amp^R P_{ADH1}::*gal4*(BD)-*divIVA*$_{Ef}$ (L104P/I115P/I125P)	This study
pMR16-AD	Amp^R P_{ADH1}::*gal4*(AD)-*divIVA*$_{Ef}$ (L104P/I115P/I25P/L143P)	This study
pMR16-BD	Amp^R P_{ADH1}::*gal4*(BD)-*divIVA*$_{Ef}$ (L104P/I115P/I25P/L143P)	This study
D. Plasmids for the studing DivIVA$_{Ef}$ in heterologous *E. coli* hosts		
pUC18	Amp^R P_{lac}::lacZ	Amersham
pUCDivWT	Amp^R P_{lac}::*divIVA*$_{Ef}$ (wild type)	This study
pUCDivMR5	Amp^R P_{lac}::*divIVA*$_{Ef}$ (E37P/N43P/L46D/L50E/L57F)	This study
pUCDivMR10	Amp^R P_{lac}::*divIVA*$_{Ef}$ (L143P)	This study
pUCDivMR16	Amp^R P_{lac}::*divIVA*$_{Ef}$ (L104P/I115P/I125P)	This study
E. Plasmids for chromosomal mutagenesis of *divIVA* and rescue assays in *E. faecalis* JH2-2		
pMSPSRDiv-2	Ery^R P_{nisA} $P_{divIVAEf}$-*divIVA*$_{Ef}$	*4*
pTCV-*lac*	Kan^R::*lacZ*	*28*
p3ERM	Ery^R P_{lac}::*lacZ*	*30*
p3ERM-kan	Ery^R Kan^R P_{aphA}::*aphA*	This study
p3ERM-kan500	Ery^R Kan^R P_{aphA}::*aphA*-500 (a 500 bp sequence immediately downstream *divIVA*$_{Ef}$	This study
pCBWT	*divIVA*$_{Ef}$ -*kan*^{R}	This study
PMWMR5	*divIVA*$_{Ef}$ (E37P/M43P/L46D/L50D/L57F)-*kan*^{R}	This study
PMWMR10	*divIVA*$_{Ef}$ (L143P)-*kan*^{R}	This study

[a]P_{ADH1}: Yeast promoter which regulates expression of *gal*4. [b]Encodes the activation domain (AD) of GAL4. [c]Encodes the DNA-binding domain (BD) of GAL4.

Table 2. **Oligonucleotide primers.**

Primer	Sequence (5′→ 3′)	RE sites[a]	Product
L29D-F	5′ GACTTTGATGATCAAAGTCACACG 3′	*Bcl*I	*divIVA*$_{Ef}$ L29D
L29D-R	5′ATCTACATCGTCTTGGTTATAGC 3′	None	
E37P-F	5′ CGTGATTATCCGGATGCATTAC 3′	*Bsp*EI	*divIVA*$_{Ef}$ E37P
E37P-R	5′ TGTGACTTGATCTAAAAAGTC 3′	None	
N43P/L46D-F	5′ CAAAAACCACGT GAAGACGAGAAATC 3′	*Bsa*AI & *Bbs*I	*divIVA*$_{Ef}$ N43P/L46D
N43P/L46D-R	5′ TAATGCATCCGATAATCACGTGTG 3′	None	
L50D/L57F-F	5′ GCAGAAGAAAAATTTCAATACTTC 3′	*Xmn*I	*divIVA*$_{Ef}$ L57F
L50D/L57F-R	5′ GTGTTTGTCTGATTTCTCGTCTTC 3′	None	*divIVA*$_{Ef}$ L46D/L50D
IVApET1	5′ GCGCCATATGGCATTAACTCCATTAGA 3′	*Nde*I	*divIVA*$_{Ef}$ 5′ end
IVApET3	5′ GCGCCTCGAGTTCCTTAACTGCTGTATG 3′	*Xho*I	*divIVA*$_{Ef}$ Δ190–233
IVA-6	5′GCGCGGATCCTTCCTTAATGCTGTATG3’	*Bam*H1	*divIVA*$_{Ef}$ Δ190–233
IVA-7	5′ GCGCCTGCAGGAAGTATTGTAATTTTTCTTC 3′	*Pst*I	*divIVA*$_{Ef}$ 1-60
IVA-10	5′GCGCCTGCAGATTGAACGTGCCCGTCAATAAG 3′	*Pst*I	*divIVA*$_{Ef}$ 130–233
IVA-8	5′ GCGCCTGCAGGAAATTCTTGATGAACAAG 3′	*Pst*I	*divIVA*$_{Ef}$ 190–233
IVA-9	5′ GCGCCTGCATAATTGCTTCTGCTAAGATTTG 3′	*Pst*I	*divIVA*$_{Ef}$ 1–130
L104P-F	5′ CCAAAGAAACCCCCGTAGAAGCTG 3′	None	*divIVA*$_{Ef}$ L104P
L104P-R	5′ CTTGGTTATCTGCCGAAGTGATAATC 3′	None	
L143P-F	5′ GAAACAGAAGACCCTAAGAAGAAAAC 3′	*Dde*I	*divIVA*$_{Ef}$ L143P
L143P-R	5′ CCCAGCTAATTGACGGGCACGTTC 3′	None	
I125P-F	5′ GAAATCAACACAACCGTTAGCAGAAGCA 3′	None	*divIVA*$_{Ef}$ I125P
I125P-R	5′ CGTTCAGCATCTGCAATCATTGC 3′	None	
I115P-F	5′ CAAATGCAATGCCCGCAGATGCTG 3′	*Aci*I	*divIVA*$_{Ef}$ I115P
I115P-R	5′ ATTTACGTTCAGCTTCTACGGGGGTTTC 3′	None	*divIVA*$_{Ef}$ L104P
IVA-1	5′ GCGCGAATTCATGGCATTAACTCCATTAGA 3′	*Eco*RI	*divIVA*$_{Ef}$ 5′ end
IVA-2	5′ GCGCGGATCCCTATTTTGATTCTTCTTCAA 3′	*Bam*HI	*divIVA*$_{Ef}$ 3′ end
IVA-6	5′ GCGCGGATCCTTCCTTAATGCTGTATG 3′	*Bam*HI	*divIVA*$_{Ef}$ 1–190
Div-fw	5′ GCGCGAATTCGATGGCATTAACTCCATTAGA 3′	*EcoR*I	*divIVA*$_{Ef}$
Div-rev	5′ GAGAGGATCCTTACTATTTTGATTCTTCTTCAA 3′	*BamH*I	*divIVA*$_{Ef}$
CBIVA-2	5′ GAGATCTAGACTATTTTGATTCTTCTTCAA 3′	*Xba*I	*divIVA*$_{Ef}$
CBkan-up	5′ GCGCTCTAGAGTGGTTTCAAAATCGGCTCCG3′	*Xba*I	P_{aphA} ~ *aphA*
CBkan-down	5′ GCGCGTCGACTAGGTACTAAAACAAATCATC3′	*Sal*I	P_{aphA} ~ *aphA*
AFdiv-up	5′ GCGCGTCGACATAGACAGAACGTTTAATGTTTATT3′	*Sal*I	500 bp downstream *divIVA*$_{Ef}$
AFdiv-down	5′ GCGCCTGCAGGAATATTTCCGTTTGCATACGG 3′	*Pst*I	500 bp downstream *divIVA*$_{Ef}$
CH-F	5′ TTCATTCAGACGAAGTTGTG 3′	None	*divIVA*$_{Ef}$~P_{aphA}~*aphA*
CH-R	5′ GAACTGCATCTAGGATAGTG 3′	None	*divIVA*$_{Ef}$~P_{aphA}~*aphA*

[a]Endonuclease restriction sites are underlined.

(Supplementary Materials; http://www.ncbi.nlm.nih.gov/sites/entrez; last accessed September 26, 2007). DivIVA protein sequences were aligned using Clustal W (http://www.ebi.ac.uk/clustalw/). Coils and Multicoil software (http://www.expasy.org) were used to identify coiled-coil domains in DivIVA$_{Ef}$. Isoelectric points (IEP) of various DivIVA$_{Ef}$ proteins were determined using EmbossIEP (http://bioweb.pasteur.fr/seqanal/interfaces/iep.html; last accessed October 10, 2007).

Polymerase Chain Reaction and DNA Sequencing—Primers (Table 2) were designed manually based on the *divIVA*$_{Ef}$ DNA sequence (EF1002; TIGR). Primer synthesis was performed either by the University of Ottawa Core DNA Sequencing and Synthesis Facility (UOCDSSF) or Invitrogen Canada (Burlington, Ontario). Polymerase Chain Reaction (PCR) reactions were performed in a Perkin-Elmer Gene Amp 9600 thermocycler (Perkin Elmer, Wellesly, MA) as previously described (*4*). DNA sequencing was performed either at the UOCDSSF or the Plant Biotechnology Institute (National Research Council Canada, Saskatoon, Saskatchewan). The *divIVA*$_{Ef}$ sequences in all constructed plasmids were verified by DNA sequence analysis.

Plasmid Construction for His-tagged DivIVA$_{Ef}$ *Expression*—To determine whether predicted coiled-coils of *E. faecalis* DivIVA play a role in oligomerization, various *divIVA* mutations were created by cloning amplicons obtained by PCR-derived site-directed mutagenesis (SDM, *24*) in pET30a or pET30a-deritives. A number of mutations predicted to disrupt the N-terminal coiled-coil were introduced into *divIVA*$_{Ef}$. To create the L29D mutation in DivIVA$_{Ef}$ (pMR1, Table 1, Panel B), primers L29D-F and L29D-R (Table 2) were used with pSRDiv (Table 1, Panel B) as template. Similarly, plasmid pMR2 (E37P) was produced by cloning SDM-generated *divIVA*$_{Ef}$ amplified using primers E37P-F and E37P-R into pSRDiv. pMR3 (E37P/N43P/L46D) was constructed using primers N43P/L46D-F and N43P/L46D-R and pMR2 as a template; pMR4 (E37P/N43P/L46D/L50D/L57F) was obtained using primers L50D/L57F-F and L50D/L57F-R and pMR3 as template. An unexpected leucine to glutamic amino acid mutation at residue 50 of DivIVA$_{Ef}$ (L50E) was found in a clone of pMR4, and this

plasmid was named pMR5 (*i.e.* mutation E37P/N43P/L46D/L50E/L57F). A *divIVA*$_{Ef}$ construct, pMR6 (Table 1, Panel B), with 43 of its C-terminal residues deleted, was constructed by PCR-amplification of pSRDiv with primers IVApET-1/IVApET-3 followed by cloning into pET30a.

Mutations or deletions in the central coiled-coil regions of *divIVA*$_{Ef}$ were also created using SDM approaches. pMR7 contained a deletion at residues 130–190 and was obtained using primers IVA-8 and IVA-9 to amplify *divIVA*$_{Ef}$ from pSRDiv followed by cloning into pET30a; pMR8 contained a deletion of residues 60–190 and was obtained using primers IVA-7 and IVA-8; pMR9 was deleted at residues 60–130 and was obtained using primers IVA-7 and IVA-10. Point mutations were also created in the predicted central coiled-coil domains of DivIVA$_{Ef}$ by SDM. Using pSRDiv as a template, the SDM amplicon obtained using primers L104P-F and L104P-R and following cloning into pET30a, generated plasmid pMR11 which contained the mutation L104P. Similarly, amplification with primers L143P-F and L143P-R produced plasmid pMR10 which contained a L143P mutation. Plasmid pMR12 contained mutations L104P and L143P and was created using pMR10 as a template and primers L104P-F and L104P-R for amplification. Similarly, pMR13 (L104P/I125P) was generated using primers I125P-F and I125P-R and pMR11 as a template; pMR14 (L104P/I125P/L143P) was created using primers I125P-F and I125P-R and pMR12 as a template. Plasmids pMR15 (L104P/I115P/I125P) and pMR16 (L104P/I115P/I125P/L143P) were created using primers I115P-F and I115P-R, and pMR13 and pMR14 as templates, respectively (Table 1, Panel B).

Protein Expression and Purification—Protein expression and purification were performed as previously reported (*4*) except for the following modifications. His-tagged DivIVA$_{Ef}$ MR6, MR9 and MR10 proteins were purified using TALON resin (Clontech) (*4*) with additional washes with 25 and 50 mM imidazole. Proteins were eluted from the TALON resin with 150 mM imidazole. Purified proteins were concentrated using a Centricon 10,000 MWCO concentrator (Millipore, Billerica, MA) and dialysed with PBS or TALON binding buffer (300 mM NaCl, 50 mM NaH_2PO_4, pH 7.0).

Protein Electrophoresis and Western Blots—DivIVA$_{Ef}$ protein purity and concentrations were analysed by sodium dodecyl sulphate polyacrylamide gel electrophoresis [SDS–PAGE; (*25*)]. 5 M urea was sometimes used in SDS–PAGE analysis. Western blots were performed using polyclonal anti-DivIVA$_{Ef}$ antibody with a modified protocol (*4*). For native gels, proteins were transferred to HybondC nitrocellulose membranes (Amersham BioScience, Montreal, QC), followed by staining with Ponceau Red (0.1% Ponceau Red, 5% acetic acid) to visualize the standard markers, and then membranes were de-stained with ddH_2O prior to antibody probing.

Mass Spectrometry Analysis—SDS–PAGE gels were stained with Coomassie brilliant blue (*25*) and purified DivIVA$_{Ef}$ bands were excised from the gel followed by de-staining in ddH_2O. MALDI–TOF Mass Spectrometry (MS) analysis was performed by the Protein Discovery Group (Queen's University, Kingston, ON).

Glycosylation Assay—The Pierce Glycoprotein staining kit (Pierce, Rockford, IL) was used to determine whether DivIVA$_{Ef}$ undergoes post-translational glycosylation.

Size Exclusion Chromatography—Gel filtration analysis (*26*) was carried out using HR16/50 Superose-6 (Amersham Biosciences, Montreal, QC) columns, packed manually according to the manufacturer's instructions which were equilibrated either with PBS or TALON binding buffer. Fractions were collected using a Pharmacia Frac-300 fraction collector (Amersham Biosciences) at 0.5–1.0 ml intervals. Chromatographic profiles were constructed as follows: 20 µl of BioRad protein assay dye (BioRad, Hercules, CA) was pipetted into each well of a 96-well microtitre plate; 100 µl of eluted protein fraction was added to each well and absorbance was recorded on a Spectra Shell microplate reader (Tecan, Maennedorf, Switzerland) at 595 nm. Molecular weight standards (Amersham Biosciences) were used to construct a plot of log MW (molecular weight) versus elution parameters (Kav) and the molecular mass of each protein was determined (*26*). The calculated protein complex mass was divided by the bioinformatically determined monomer mass (27.4 kDa for 6XHis-tagged wild-type DivIVA$_{Ef}$) of the protein to derive the number of DivIVA$_{Ef}$ monomers in the complex.

Native Gel Electrophoresis—Gradient Tris–HCl gels were purchased from BioRad. Loading buffer (40% glycerol, 0.01% bromophenol blue, 62.5 mM Tris–HCl pH 6.8) was added to purified protein samples in a 1 : 5 ratio. Electrophoresis was conducted in a solution of 192 mM glycine and 25 mM Tris–HCl pH 8.3 at 100 V.

Yeast Two-Hybrid Assays—Wild-type and mutated *divIVA*$_{Ef}$ were PCR amplified using primers IVA-1 and IVA-2 (Table 2) and templates pMR1 to pMR16 (Table 1, Panel C). The various *divIVA*$_{Ef}$ amplicons were cloned (Table 1) into the Y2H vectors pGAD424 and pGBT9 (Clontech, Mountain, California, USA). A C-terminal truncation in *divIVA*$_{Ef}$ was also amplified using primers IVA-1 and IVA-6 and pSRDiv as template. Y2H plasmid constructs were transformed, either singly or in pairs, into *S. cerevisiae* SFY526. Assays for β-galactosidase activity were performed as described by the manufacturer (Clontech).

Expression of DivIVA$_{Ef}$ Mutations in Escherichia coli Hosts—To determine whether mutations in DivIVA$_{Ef}$ would interfere with cell division, round (KJB24, *rodA*) or rod-shaped (PB103) *E. coli* cells were used as heterologous hosts for overexpression of the various proteins. Wild-type DivIVA$_{Ef}$ and DivIVA$_{Ef}$ mutations MR5 (E37P/N43P/L46D/L50E/L57F), MR10 (L143P) and MR15 (L104P/I115P/I125P) were selected to represent the disruptions of the N-terminal (MR5) and different (MR10 or MR15) central coiled-coil regions. Wild-type *divIVA*$_{Ef}$ and *divIVA*$_{Ef}$ MR5, MR10 or MR15 were PCR-amplified with primers Div-fw and Div-rev. *Enterococcus faecalis* chromosomal DNA was used as a PCR template for amplification of the wild-type *divIVA*, and plasmids pMR5 (E37P/N43P/L46D/L50E/L57F), pMR10 (L143P) and pMR15 (L104P/I115P/I125P) were used as templates to amplify mutated *divIVA*$_{Ef}$. Each amplicon was cloned into pUC18, producing plasmids pUCDiv-WT, pUCDiv-MR5, pUCDiv-MR10 and pUCDivMR15, respectively

(Table 1, Panel D). Plasmid constructs were confirmed by restriction endonuclease digestion and DNA sequence analysis and were separately transformed into either *E. coli* KJB24 or PB103. After optimizing the expression levels of the DivIVA$_{Ef}$ proteins in western blots, cells were harvested for observation by light microscopy (*i.e*. differential interference contrast, DIC) as described previously (*4*, *27*). Approximately 500–1000 cells were counted in consecutive microscopic fields, and each experiment was performed twice. Western blot assays were performed as described previously.

Creation of Mutations in Enterococcus faecalis divIVA$_{Ef}$—Plasmid constructs containing the sequences '*divIVA*$_{Ef}$ (or mutant)- kan^R - 500 bp downstream of *divIVA*$_{Ef}$' were developed to create strains of *E. faecalis* containing chromosomal mutations in *divIVA* produced by homologous recombination. First *divIVA$_{Ef}$* amplicons containing various mutations were PCR-amplified with primers IVA-5/CBIVA-2 using pMR5 (E37P/N43P/L46D/L50E/L57F) and pMR10 (L143P) as templates. Wild-type *divIVA*$_{Ef}$ was amplified from *E. faecalis* JH2-2. The *kan^R* cassette (*28*) was PCR-amplified from pTCV-*lac* with primers CBkan-up and CBkan-down and the 500 bp sequence immediately downstream *divIVA*$_{Ef}$ in *E. faecalis* JH2-2 was PCR-amplified using primers AFdiv-up and AFdiv-down. The three amplicons (*i.e*. *divIVA*$_{Ef}$, *kan^R* cassette and 500 bp downstream sequence) were cloned into suicide vector p3ERM (*29*) sequentially. These constructs (Table 1, Panel E) were named pCBWT (wild-type DivIVA$_{Ef}$), pMWMR5 (DivIVA$_{Ef}$ mutation E37P/N43P/L46D/L50E/L57F) and pMWMR10 (DivIVA$_{Ef}$ mutation L143P). The entire *divIVA* DNA sequence was verified for each construct. Plasmids were individually transformed into *E. faecalis* JH2-2 as previously described (*4*, *30*). After several trials, no transformed colonies were obtained with pMWMR5 or pMWMR10, suggesting that the mutations in *divIVA* obtained through homologous recombination were lethal to the host strain. Colonies were obtained with each pCBWT transformation.

Rescue experiments were performed to express wild-type *divIVA*$_{Ef}$ *in trans*. The *divIVA*$_{Ef}$ shuttle vector pMSPSRDiv-2 (erythromycin resistant) containing wild-type *divIVA*$_{Ef}$ under the control of its native promoter was constructed previously (*4*). Plasmid pMWMR5 or pMWMR10 was co-transformed into *E. faecalis* JH2-2 with pMSPSRDiv-2 with selection on erythromycin and kanamycin. *divIVA*$_{Ef}$ mutations by homologous recombination were confirmed by DNA sequence analysis of PCR amplicons using primers CH-F and CH-R (Table 2). The *E. faecalis* mutants (Table 1, Panel A) were named CBWT (wild-type *divIVA*), MWMR5 (E37P/N43P/L46D/L50E/L57F) and MWMR10 (L143P). These strains carried a *kan^R* cassette downstream of *divIVA*; *E. faecalis* MWMR5 and MWMR10 also harboured plasmid pMSPSRDiv-2.

Effects of Mutations in DivIVA on the Phenotype of Enterococcus faecalis—E. faecalis strains JH2-2, JH2-2+R, CBWT, MWMR5 and MWMR10 were cultured in BHI medium with or without antibiotics (Kan 1,000 μg/ml, Ery 125 μg/ml or Kan 50 μg/ml plus Ery 125 μg/ml) (*4*). Cells were incubated without agitation at 37°C either overnight (~20 h) to stationary phase, or for 8 h to log phase. Cells were harvested and fixed for light microscopy as described previously (*4*). Over 500 cells for each strain were examined in consecutive microscopic fields. Each experiment was performed twice.

Transmission electron microscopy (TEM) was also performed on cells in stationary phase to observe *E. faecalis* cell morphology, as described previously (*4*), using a Hitachi Transmission Electron Microscope H-7000 (Electron Microscopy Unit, Surgical Medical Research Institute, University of Alberta, Edmonton, Alberta). The shape of a septating cell was defined by measuring the ratio of the two axes, or the pole-to-pole length (x) versus the length between the two dividing sites (y). Cells with an $x/y \leq 1.50$ were considered to be spherical in shape; otherwise they were counted as being more lancet-shaped. Percentages of cells with different shapes were calculated based on the examination of 40–60 cells.

RESULTS

Prediction of DivIVA$_{Ef}$ Coiled-coil Domains—Multiple sequence alignments indicated that among the 27 DivIVA protein sequences (Supplementary Materials, Fig. A) the N-terminus [amino acids (AA) M1 to T94 of DivIVA$_{Ef}$] was most conserved. DivIVA proteins from *E. faecalis*, *B. subtilis*, *S. pneumoniae* and *S. aureus* carried a highly conserved N-terminal coiled-coil domain. An N-terminal coiled-coil domain was also predicted in DivIVA from *Clostridium perfringens*, *Cytophaga hutchinsonii*, *Geobacillus kaustophilus*, *Lactobacillus acidophilus*, *Listeria innocua*, *M. xanthus*, *Oceanobacillus iheyensis*, *Symbiobacterium thermophilum* and *Thermoanaerobacter tengcongensis* (data not shown). The central region (AA S95 to K175 of DivIVA$_{Ef}$) was moderately conserved while the C-terminus (AA P176 to K233 of DivIVA$_{Ef}$) was least conserved. DivIVA$_{Ef}$ contains four predicted coiled-coil structures, one in the N-terminus (AA24-70), two in the central region (AA98–121 and AA115–146, respectively) and one in the C-terminus (AA180–200) (Supplementary Materials, Fig. A and B-a). In comparison, DivIVA from *B. subtilis* contained only two predicted coiled-coil structures, one in the N-terminus and one in the central region (data not shown).

Discrepancy between the Observed and Predicted Molecular Weight of DivIVA$_{Ef}$—While the molecular weights for the native and the 6XHis-tagged DivIVA$_{Ef}$ were predicted to be ~26.64 and 27.4 kDa, respectively (data not shown), the mobility of purified 6XHis-tagged DivIVA$_{Ef}$ in SDS–PAGE gels corresponded to a mass of ~40 kDa (Fig. 1). Two bands were detected in SDS–PAGE (Fig. 1). Proteins from both bands were identified as DivIVA$_{Ef}$ by MALDI–TOF analysis (data not shown). Western blot analysis using DivIVA$_{Ef}$ antiserum (*4*) demonstrated that purified DivIVA$_{Ef}$ migrated identically to anti-DivIVA$_{Ef}$ from *E. faecalis* cell lysates (data not shown). Purified DivIVA$_{Ef}$ was further examined by urea SDS–PAGE and no change in mobility was observed, as compared to standard SDS–PAGE (data not shown). Furthermore, glycosylation assays indicated that DivIVA$_{Ef}$ was not modified by post-translational

glycosylation (data not shown). Aberrant electrophoretic mobilities were observed for $DivIVA_{Ef}$ that had been either truncated or deleted (MR6, MR7 and MR9; Table 3). The IEP for wild-type $DivIVA_{Ef}$, or $DivIVA_{Ef}$ MR6 (Δ191–232), MR7 (Δ130–190) and MR9 (Δ60–130) were calculated along with the predicted net charge for each protein at pH 8.5 (Table 3). A comparison of the amount of aberrant mobility to the charge of each protein showed that, as the charge decreased, the percentage of aberrant migration also decreased (Table 3).

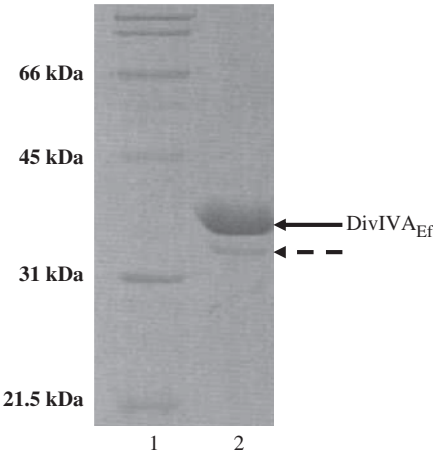

Fig. 1. **$DivIVA_{Ef}$ mobility by SDS–PAGE.** Proteins were separated on 12% SDS–PAGE. Lane 1-protein molecular weight markers; Lane 2-purified $DivIVA_{Ef}$ stained with Coomassie blue. A small portion of purified $DivIVA_{Ef}$ (dashed arrow) ran slightly faster.

Wild-type $DivIVA_{Ef}$ Forms a Multimeric Complex In Vitro—Purified wild-type $DivIVA_{Ef}$ formed a large protein complex with an elution profile similar to the thyroglobulin (669 kDa) standard in size exclusion chromatography (SEC) analysis (Fig. 2, open arrow). Based on a bioinformatically predicted monomer mass of 27.4 kDa for 6XHis-$DivIVA_{Ef}$, this complex therefore comprised ~25 $DivIVA_{Ef}$ monomers. In Native Gel Electrophoresis (NGE), the 6XHis-fused wild-type $DivIVA_{Ef}$ migrated to a position corresponding to a mass size of ~288 kDa (Fig. 3, Lane 2), comprising approximately 10 monomers as determined by the predicted molecular weight of 6XHis-$DivIVA_{Ef}$.

N-terminal Coiled-coil of $DivIVA_{Ef}$ is not Implicated in Oligomerization—$DivIVA_{Ef}$ proteins MR1 to MR5

Table 3. **Comparison between aberrant mobility on SDS-PAGE and predicted protein charge for wild-type and deletion mutants of $DivIVA_{Ef}$.**

$DivIVA_{Ef}$ proteins	Predicted molecular weight (kDa)	Observed molecular weight (kDa)[a]	Predicted charge at pH 8.5	Percent aberrant migration[b] (%)
Wild type (1–233)	26.64	39.46	−24.62	48.12
MR7 (Δ130–190)	19.68	33.54	−24.58	70.43
MR9 (Δ60–130)	19.20	28.00	−19.59	45.83
MR6 (Δ190–233)	21.75	30.09	−11.61	38.37

[a]Mass was calculated based on eletrophoretic mobility of standards. [b]Percent aberrant migration = (observed molecular weight−predicted molecular weight)/predicted molecular weight.

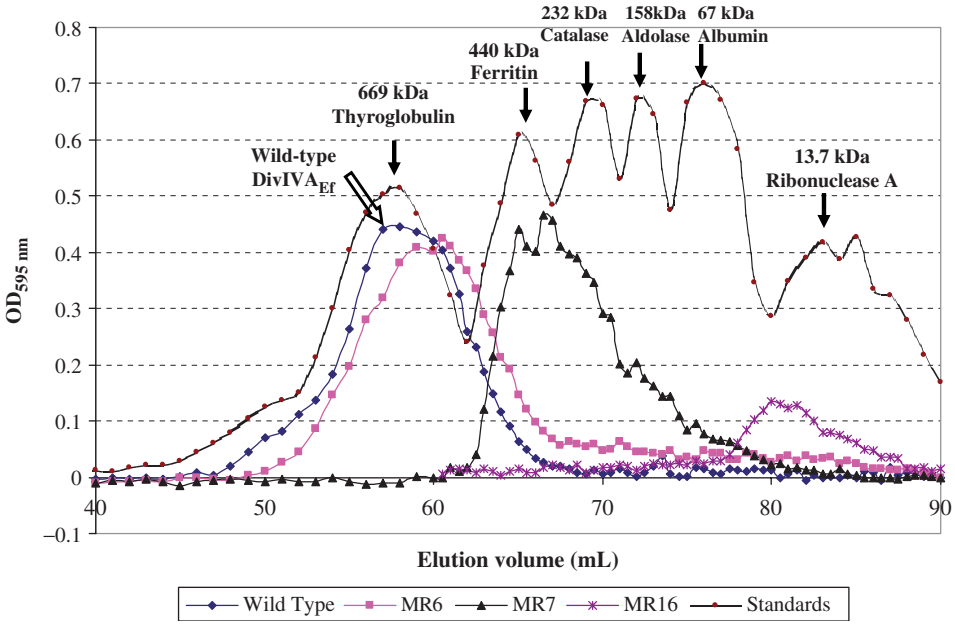

Fig. 2. **Elution profiles of $DivIVA_{Ef}$ proteins using Superose-6 size exclusion chromatography.** Because purified 6XHis-tagged $DivIVA_{Ef}$ MR1 to MR5 proteins displayed an elution profile identical to wild-type $DivIVA_{Ef}$, only the wild-type $DivIVA_{Ef}$ profile is shown (open arrow). The elution profiles of $DivIVA_{Ef}$ MR6 and MR7 are represented by purple squares and black triangles, respectively. $DivIVA_{Ef}$ MR12 to MR16 exhibited similar elution profiles, and only the $DivIVA_{Ef}$ MR16 profile is shown (brown stars). Molecular weight standards (brown dots) are indicated by black arrows and include thyroglobulin (669 kDa), ferritin (440 kDa), catalase (232 kDa), aldolase (158 kDa), albumin (67 kDa) and RNase A (13.7 kDa). The column void volume and column volume were ~30 ml and ~100 ml, respectively. Flow rate was maintained at 0.7 ml/min. The sample volume is ~0.5 ml.

contained mutations predicated to disrupt its N-terminal coiled-coil domain (Table 1, Panel B, Supplementary Materials Fig. B-b). Each of the purified $DivIVA_{Ef}$ proteins MR1 to MR5 had a similar elution profile to wild-type $DivIVA_{Ef}$, as determined by SEC (Table 4). These mutated proteins migrated similarly in NGE as a 10–12 mer protein complex (only MR 5 is shown; Fig. 3, Lane 8).

C-terminal Coiled-coil Domain of $DivIVA_{Ef}$ is not Involved in Oligomer Formation—$DivIVA_{Ef}$ MR6 (Δ190–233) was eluted at a position between the thyroglobulin (669 kDa) and ferritin (440 kDa) standards (Fig. 2). The calculated mass size was ∼580 kDa, comprising ∼25 monomers (Table 4). MR6 migrated as a mass of about 180 kDa comprising ∼8 monomers (Fig. 3, Lane 9).

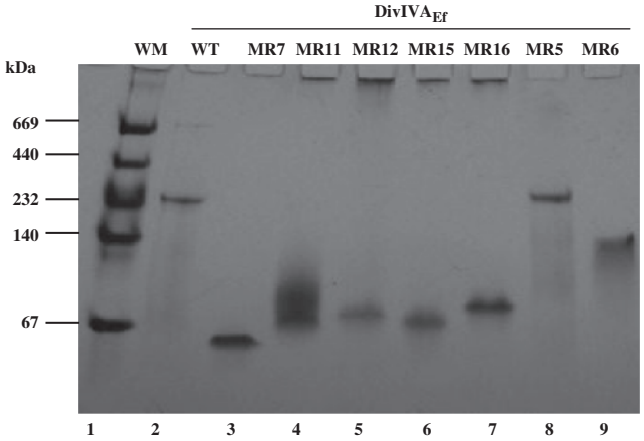

Fig. 3. **Native gel electrophoresis of $DivIVA_{Ef}$ proteins.** Lane 1—protein molecular weight markers; molecular weight (kDa) of each band was indicated on the left; Lane 2—wild-type $DivIVA_{Ef}$; Lane 3—$DivIVA_{Ef}$ MR7, Lane 4—$DivIVA_{Ef}$ MR11, Lane 5—$DivIVA_{Ef}$ MR12, Lane 6—$DivIVA_{Ef}$ MR15, Lane 7—$DivIVA_{Ef}$ MR16, Lane 8—$DivIVA_{Ef}$ MR5, Lane 9—$DivIVA_{Ef}$ MR6.

Disruption of the Central Coiled-coil Domains Affected Oligomerization—The central region of $DiIVA_{Ef}$ carries two predicted coiled-coil domains (Supplementary Materials, Fig. B). Both $DivIVA_{Ef}$ MR7 (Δ130–190) and MR9 (Δ60–130) lack one of the two coiled-coil structures in the central region (data not shown). $DivIVA_{Ef}$ MR7 eluted as a mass of ∼260 kDa in SEC (Fig. 2) comprising approximately 12 monomers (Table 4) and migrated in NGE as a mass of ∼52 kDa (Fig. 3, Lane 3) comprising ∼2.4 monomers (Table 4). MR9 migrated in NGE as a 59 kDa complex comprising ∼3 monomers (data not shown); however, SEC analysis for MR9 was not performed since a high protein concentration could not be obtained.

To identify which amino acids in the central coiled-coil regions were implicated in $DivIVA_{Ef}$ oligomerization, various point mutations were created by SDM to disrupt the central coiled-coils (MR10–MR16; Table 1). These seven purified proteins were analysed by SEC, NGE or both. MR10 (L143P; Supplementary Materials, Fig. B-c) was predicted to disrupt the second coiled-coil, and it migrated as a 91 kDa mass comprising ∼4 monomers in NGE (Table 4, data not shown in Fig. 3) (Table 4). MR10 could not be analysed by SEC because sufficiently concentrated protein was not obtained. MR11 (L104P) was predicted to partially disrupt the first coiled-coil in the central region (data not shown) and it exhibited a large complex similar to wild-type $DivIVA_{Ef}$, in SEC analysis, comprising ∼25 monomers (Table 4). In NGE analysis, MR11 migrated as two species (Fig. 3, Lane 4)—the major band had a mass size of 125 kDa comprising 4.6 monomers and the minor band exhibited a mass of 78 kDa with ∼2.8 monomers. MR12 (L104P/L143P) was predicted to partially disrupt the first and second coiled-coil in the central region (data not shown), and it eluted as a 67 kDa complex in SEC (data not shown) comprising 2.4 monomers (Table 4). MR12 migrated as a 64.2 kDa mass in NGE (Fig. 3, Lane 5) comprising 2.4 monomers (Table 4). MR13 (L104P/I115P) was predicted to partially disrupt the first coiled-coil in the central

Table 4. **The association of $DivIVA_{Ef}$ mutations and protein oligomerization.**

$DivIVA_{Ef}$ Proteins	Mutation/Truncation	SEC[a] (kDa/No. of monomers)	NGE[b] (kDa/No. of monomers)
WT[c]	None	669/25	288/10
MR1	L29D	669/25	299/11
MR2	E37P	669/25	332/12
MR3	E37P/N43P/L46D	669/25	344/12
MR4	E37P/N43P/L46D/L50D/L57F	669/25	332/12
MR5	E37P/N43P/L46D/L50E/L57F	669/25	332/12
MR6	Δ190–233	580/25	182/8
MR7	Δ130–190	260/12	52/2.4
MR9	Δ60–130	ND[d]	59/3
MR10	L143P	ND	91/4
MR11	L104P	669/25	125/4.6 and 78/2.8
MR12	L104P/L143P	66.9/2.4	64.2/2.4
MR13	L104P/I125P	29.9/1.1	64.2/2.4
MR14	L104P/I125P/L143P	100/3.7 and 28.9/1	69.8/2.6
MR15	L104P/I115P/I125P	27/1.0	61.6/2.3
MR16	L104P/I115P/I125P/L143P	40.4/1.5	66.9/2.5

[a]SEC, size exclusion chromatography. Number of monomers were calculated by mass size divided by predicated molecular weight of a monomer. [b]NGE, native gel electrophoresis. Number of monomers were calculated by mass size divided by predicated molecular weight of a monomer. [c]WT, 6XHis-fused wild type $DivIVA_{Ef}$, predicted molecular weight 27.4 kDa. [d]ND, not determined.

region (data not shown), and it eluted as a 30 kDa complex in SEC (data not shown) comprising 1.1 monomers, it migrated similar to MR12 in NGE (data not shown) comprising 2.4 monomers (Table 4). MR14 (L104P/I115P/L143P) was predicted to partially disrupt the first and the second coiled-coils in the central region, and it eluted as two species in SEC –100 kDa (~3.7 monomers) and 29 kDa (~1 monomer) (Table 4). By NGE, MR14 migrated as a 29.8-kDa mass (~2.6 monomers) (data not shown). MR15 (l104P/I115P/I125P; Supplementary Materials, Fig. B-d) was predicted to completely disrupt the first coiled-coil of the central region. MR15 eluted as a mass of 27 kDa in SEC representing 1 monomer (Table 4), and it migrated as a 61.6 kDa mass in NGE (Fig. 4, Lane 6) comprising ~2.3 monomers (Table 4). MR16 (l104P/I115P/I125P/L143P; Supplementary Materials, Fig. B-e) was predicted to completely disrupt both coiled-coils in the central region. MR16 eluted as a 40 kDa mass (Fig. 2) comprising ~1.5 monomers (Table 4), it migrated as a 66.9 kDa mass in NGE (Fig. 3, Lane 7) comprising ~2.5 monomers (Table 4).

Wild-type $DivIVA_{Ef}$ strongly self-interacts in Y2H experiments (Table 5). $DivIVA_{Ef}$ MR1 to MR5, comprising N-terminal mutations self-interacted, as determined by Y2H colony lift assays, but their interaction strength was significantly decreased as compared to wild-type $DivIVA_{Ef}$ self-interaction (Table 5). $DivIVA_{Ef}$ MR6, with a C-terminal truncation exhibited self-interaction in Y2H assays, comparable to wild-type $DivIVA_{Ef}$ (Table 5). No self-interactions were detected between $DivIVA_{Ef}$ containing mutations in the central coiled-coil domains (*i.e.* MR10, 12, 15 and 16). Two $DivIVA_{Ef}$ mutated proteins MR7 (Δ130–190) and MR 9 (Δ 60–130) had self-activating activities when fused with GAL4 DNA binding domain (DBD) in the Y2H vector; therefore, their self interaction could not be determined. When MR7 and MR9 were fused to GAL4 activation domain (AD), they interacted with the wild-type $DivIVA_{Ef}$ which was fused to the GAL4 DBD domain in the Y2H assays. $DivIVA_{Ef}$

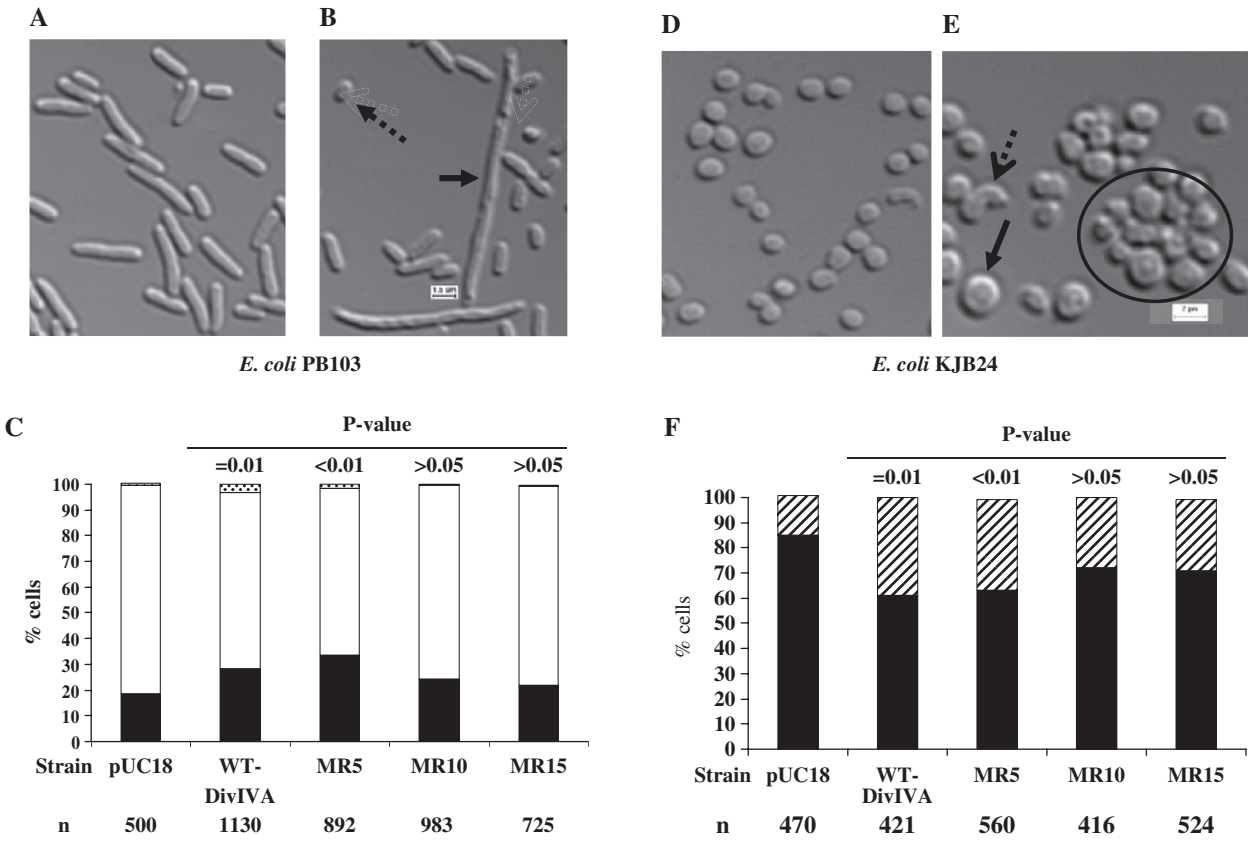

Fig. 4. **Expression of $DiIVA_{Ef}$ *Escherichia coli* PB103 and KJB24.** Differential interference contrast (DIC) images showing the phenotypes of *E. coli* PB103 carrying pUC18 (A) and overexpressing wild-type $DivIVA_{Ef}$ from pUCDivWT (B). Closed arrow shows an elongated cell and dashed arrow shows cells smaller than 1.5 μm in length. (C). Phenotypes of *E.coli* PB103 overexpressing wild-type $DivIVA_{Ef}$ and $DivIVA_{Ef}$ MR5, MR10 and MR15. Approximately 500–1100 cells are counted for each strain. Black bars: % cells <1.5 μm in length; white bars: % cells with 'normal' length (1.5–4.5 μm); hatched bars: % cells >4.5 μm in length. (D). DIC image of *E. coli* KJB24 cells transformed with pUC18. (E). (DIC) image of *E. coli* KJB24 cells overexpressing wild-type $DivIVA_{Ef}$. Closed arrow indicates a round enlarged cell; dashed arrow shows a cell with irregular shape; circle indicates a clump of cells. The scale bar represents 2 μm. (F). Phenotypes of *E. coli* KB104 overexpressing wild-type $DivIVA_{Ef}$, MR5, MR10 and MR15. Black bars: % cells with typical *E. coli* KJB24 morphology; hatched bars: % cells with irregular shapes and enlarged cells (diameter >1.5 μm). 'n' in (C) and (F) represents number of cells counted for each *E. coli* strain. *P*-values are calculated using the chi-square test comparing cells expressing wild-type $DivIVA_{Ef}$ or mutated $DivIVA_{Ef}$ to cells carrying pUC18. A *P*-value of < 0.05 is considered significant.

Table 5. **The yeast two-hybrid analysis of DivIVA$_{Ef}$ protein interactions.**

DivIVA$_{Ef}$ protein	Mutations	Colony lift assay		ONPG liquid assay
		Self-interaction	Interaction with WT DivIVA$_{Ef}$	β-galactosidase activity (units)
WT[a]	None	Positive	ND[b]	29.25 ± 6.70
MR1	L29D	Positive	ND	2.64 ± 1.16
MR2	E37P	Positive	ND	17.53 ± 0.52
MR3	E37P/N43P/L46D	Positive	ND	7.36 ± 0.72
MR4	E37P/N43P/L46D/L50D/L57F	Positive	ND	7.83 ± 1.50
MR5	E37P/N43P/L46D/L50E/L57F	Positive	ND	8.69 ± 1.20
MR6	Δ190–233	Positive	ND	23.65 ± 1.54
MR7	Δ130–190	ND	Positive	ND
MR9	Δ60–130	ND	Positive	ND
MR10	L143P	Negative	Positive	ND
MR12	L104P/L143P	Negative	Positive	ND
MR15	L104P/I115P/I125P	Negative	Positive	ND
MR16	L104P/I115P/I125P/L143P	Negative	Negative	ND

[a]WT, wild type. [b]ND, not determined.

mutations MR10, MR12 and MR15 interacted with wild-type DivIVA$_{Ef}$, whereas DivIVA$_{Ef}$ MR16 did not (Table 5).

Overexpression of DivIVA$_{Ef}$ Mutations in Escherichia coli—We had previously shown that *E. coli* was a useful heterologous host for studying the effects of the overexpression of DivIVA$_{Ef}$ (*4*). Accordingly, both 'round' and rod-shaped *E. coli* were used as heterologous hosts for the expression of DivIVA and its mutated proteins. The effects of DivIVA$_{Ef}$ overexpression in rod-shaped *E. coli* PB103 is shown in Fig. 4. In comparison to cells carrying pUC18 (Fig. 4A), cells overexpressing wild-type DivIVA$_{Ef}$ or DivIVA$_{Ef}$ MR5 had significantly higher percentages of aberrant cells. The aberrant phenotypes upon overexpression of wild-type DivIVA$_{Ef}$ and DivIVA$_{Ef}$ MR5 (E37P/N43P/L46D/L50E/L57F) included elongation and filamentation accompanied by cells of shorter length (Fig. 4B). In contrast, the overexpression of DivIVA$_{Ef}$ MR10 (L143P) or MR15 (l104P/I115P/I125P) did not alter cell phenotypes as compared to cells carrying the pUC18 vector (Fig. 4C). DivIVA$_{Ef}$ overexpression was confirmed by western blot analysis for all constructs (data not shown).

Wild-type DivIVA$_{Ef}$ also had significant morphological impact when overexpressed in *E. coli* KJB24 (Fig. 4D), producing cell clumps, cell death and irregular/asymmetrically-shaped cells (Fig. 4E). The DivIVA$_{Ef}$ N-terminal mutation MR5 produced the same morphological changes as wild-type DivIVA$_{Ef}$ when overexpressed in *E. coli* KJB24. In contrast, overexpression in *E. coli* KJB24 of DivIVA$_{Ef}$ MR10 or MR15 did not produce obvious morphological changes (Fig. 4F). DivIVA$_{Ef}$ overexpression in these cells was confirmed by western blot analysis (data not shown).

Effects of Expressing DivIVA$_{Ef}$ Mutations in Enterococcus faecalis—To investigate the effects of disrupting the coiled-coil domains on the biological function of DivIVA$_{Ef}$ in *E. faecalis* JH2-2 backgrounds, various mutations were introduced by homologous recombination. Several attempts to obtain viable *E. faecalis* cells containing *divIVA*$_{Ef}$ mutations which disrupted the N-terminal (MR5) or the central (MR10) coiled-coil structures were unsuccessful, possibly indicating that these mutations were lethal. Therefore, rescue experiments were performed to express wild-type DivIVA$_{Ef}$ *in trans*.

Enterococcus faecalis strains CBWT, MWMR5 and MWMR10 (Table 1) were examined by TEM. *Enterococcus faecalis* JH2-2 cells were characterized as lancet-shaped diplococci with symmetrical division at the mid-cell (data not shown). Over 80% of *E. faecalis* CBWT cells exhibited morphology typical of *E. faecalis* JH2-2 cells (Fig. 5A). *Enterococcus faecalis* MWMR5 (Fig. 5B) and MWMR10 (Fig. 5C) exhibited altered morphology in over 80% of the cells with most appearing as spherical (~70%) or with asymmetrical division (1–2%, arrowheads in Fig. 5B) or improper separation (~8%, arrows in Fig. 5B and C). Percentages of cells with altered morphology in *E. faecalis* MWMR5 and MWMR10 were significantly higher than for *E. faecalis* JH2-2 or CBWT (Fig. 5D).

As observed by DIC light microscopy (Fig. 5E), *E. faecalis* JH2-2 cells exhibited typical morphology, were 0.8–1 μm in diameter, and appeared as pairs or short chains at either log or stationary growth phase (*4*). *Enterococcus faecalis* CBWT or JH2-2+R cells displayed similar morphology indicating that the insertion of a *kan*^{R} cassette or DivIVA expressed from the plasmid pMSPSRDiv-2 did not induce morphological alterations, as noted previously (*4*). About 50% of *E. faecalis* MWMR5 and MWMR10 cells exhibited aberrant morphology, as characterized by either an enlarged spherical shape or irregular shapes or aggregates (data not shown), while very few *E. faecalis* JH2-2, JH2-2+R or CBWT cells exhibited such morphologies.

DISCUSSION

Structural predictions indicate that DivIVA, a cell division protein of Gram positive bacteria, has a predominantly coiled-coil structure (*2*). *Enterococcus faecalis* DivIVA comprises four coiled-coil domains, one at the N-terminus, two in the central region of the protein and one at the C-terminus (Supplementary Materials). Coiled-coil

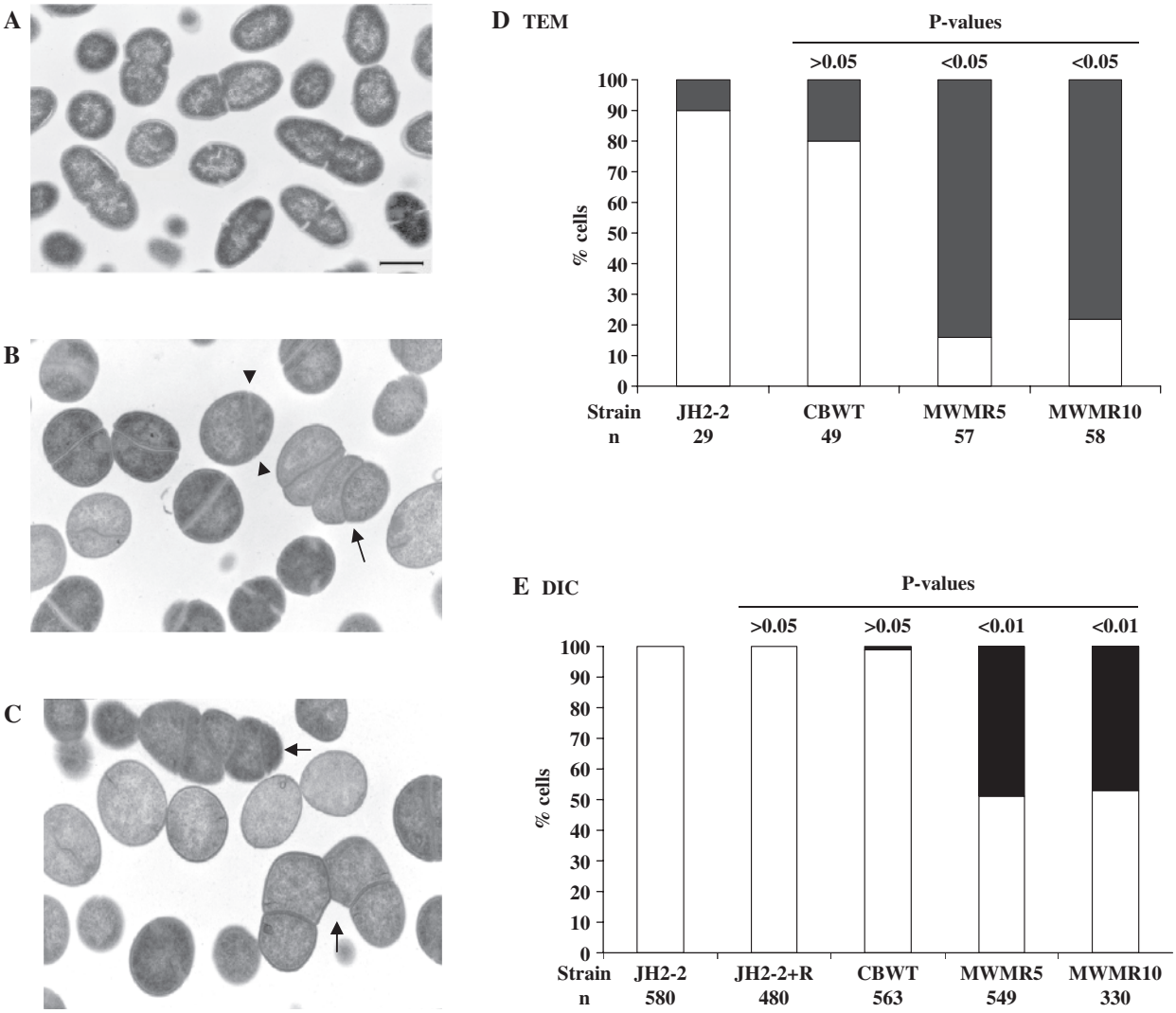

Fig. 5. **Expression of *Enterococcus faecalis divIVA* mutants by transmission electron microscopy (TEM) and differential interference contrast (DIC) light microscopy.** TEM images of *E. faecalis* CBWT (A), MWMR5 (B) and MWMR10 (C) are shown. Arrows indicate short chains of several cells (B and C); arrowheads indicate asymmetrical division of *E. faecalis* MWMR5 (B). Images A, B and C are of the same magnification, and scale bar in A represents 1 micron. (D). Percentages of *E. faecalis* strains by TEM; White bars —% cells with lancet shape diplococci; Black bars—% cells with aberrant morphology (spherical, short chain and asymmetrical division). (E). Percentages of *E. faecalis* strains by DIC. White bars—lancet shaped diplococci, white bars—aberrant morphology (enlarged spheres, short chains, and irregular shapes). 'n' represents number of cells counted for each strain (D and E). *P*-values are calculated using the chi-square test comparing *E. faecalis* mutants to JH2-2. A *P*-value of < 0.05 is considered significant.

structures are implicated in the dimerization/oligomerization of many different proteins and in interactions with other proteins (*2*, *14*, *31*, *32*). Our research establishes that $DivIVA_{Ef}$ oligomerizes *in vitro*, forming a complex containing 10–12 monomers. Oligomer formation of $DivIVA_{Ef}$ requires the central coiled-coil domains. Specific amino acids were predicted to be important for the maintenance of the coiled-coil structures in $DivIVA_{Ef}$ and for the formation of oligomer complexes. A single L143P point mutation in $DivIVA_{Ef}$ (MR10) was predicted to disrupt the second coiled-coil domain in the central region (Supplementary Materials). $DivIVA_{Ef}$ MR10 was not able to form a 10–12 mer protein complex, instead forming a 4-mer, supporting the importance of this conserved leucine residue in $DivIVA_{Ef}$ in oligomer formation. The corresponding mutation of *B. subtilis* $DivIVA_{Bs}$ (L120P) also resulted in a reduction in the size of the $DivIVA_{Bs}$ complex (*17*). Three simultaneous point mutations ($DivIVA_{Ef}$ MR15, L104P/I115P/I125P) aimed at disrupting the first coiled-coil domain of the central region produced a monomeric $DivIVA_{Ef}$ protein. However $DivIVA_{Ef}$ MR15 retained its ability to interact with wild-type $DivIVA_{Ef}$ as determined in Y2H assays, indicating that this coiled-coil domain is important, but may not be sufficient for mediating $DivIVA_{Ef}$ self-association. More extensive mutations in the central coiled-coil region ($DivIVA_{Ef}$ MR16) which disrupted both coiled-coil domains of $DivIVA_{Ef}$ abolished both the ability of the mutated protein to self-associate and

its ability to interact with wild-type DivIVA$_{Ef}$. Mutations or truncations disrupting N-terminal or C-terminal coiled-coil structures of DivIVA$_{Ef}$ did not affect self-interaction and oligomerization. Thus we conclude that the central coiled-coil structures are essential and sufficient for the formation of a DivIVA$_{Ef}$ oligomer. Under this reasoning, DivIVA$_{Ef}$ with the central region deleted (DivIVA$_{Ef}$ MR6, MR7 and MR9) should not be able to self-interact, a hypothesis confirmed by Y2H assays. Interestingly, both DivIVA$_{Ef}$ MR7 and MR9 proteins retained the ability to interact with wild-type DivIVA$_{Ef}$. This effect could be due to conformational changes caused by these deletions, exposing buried domains which might mediate association.

Although the N-terminal mutations of DivIVA$_{Ef}$ MR1-MR5 did not seem to alter the size of the protein complex, as determined by SEC and NGE, their strength of their self-association was greatly reduced in Y2H assays. A difference between the calculated monomer content obtained by SEC as compared to NGE analysis was noted in our studies. This discrepancy in DivIVA$_{Ef}$ complex size between SEC and NGE might be caused by the shape of the protein. The size calculation for SEC analysis was based on 'spherical' standard proteins (*26*). However, DivIVA most likely forms secondary structures which are not spherical (*19*), thereby producing earlier elution from SEC columns. DivIVA$_{Ef}$ had a lower than expected mobility in SDS–PAGE, resulting in an observed molecular weight higher than predicted through bioinformatic analysis. Such aberrant SDS–PAGE mobility also has been observed for a number of other proteins (*33–36*), and we have also noted this for *S. epidermidis* DivIVA (data not shown). Factors contributing to such aberrant mobility (*36*) could include post-translational modifications, incomplete disulphide bond reduction, excessive positive or negative charge, or association of globular domains through flexible linkers containing unusual amino acid compositions. Analysis of the predicted protein charge of DivIVA$_{Ef}$ and the deletion constructs DivIVA$_{Ef}$ MR6 (Δ190–233), MR7 (Δ130–190) and MR9 (Δ60–130) demonstrated that as the charge on the protein decreased, the electrophoretic mobility became less aberrant. This suggests that charge may play a role in DivIVA$_{Ef}$ migration. Post-translational modification of DivIVA$_{Ef}$, such as tyrosine phosphorylation, may also contribute to the slower SDS–PAGE migration. Protein phosphorylation occurs in a number of bacterial species and appears to be ubiquitous among prokaryotes (*37*). The *Mycobacterium tuberculosis* DivIVA homologue, Wag31, has been shown to be phosphorylated and this affected its function and SDS–PAGE migration (*38*).

The biological impact of abolishing the DivIVA$_{Ef}$ coiled-coil structures was investigated in an *E. faecalis* background. Construction of *E. faecalis divIVA* mutants (*E. faecalis* MWMR5-E37P/N43P/L46D/L50E/L57F and MWMR10-L143P) were successful only by co-transforming a rescue vector that expressed wild-type DivIVA$_{Ef}$ *in trans*, indicating that the N-terminal and the central coiled-coil domains are essential for DivIVA$_{Ef}$ biological function. Interestingly, wild-type *divIVA*$_{Ef}$ expressed from the rescue plasmid failed to completely compensate for the deleterious effects caused by the mutations, in agreement with our previous observations (*4*). One explanation is that the expression levels of the wild-type *divIVA* were not the same as those from the wild-type *E. faecalis* JH2-2 cells (*4*). In addition, wild-type DivIVA$_{Ef}$ expression from the plasmid may have been sequestered by interaction with DivIVA$_{Ef}$ mutated proteins MR10 or MR15; these mutated proteins retained an ability to interact with wild-type DivIVA$_{Ef}$, as determined in Y2H assays.

E. faecalis containing an N-terminal mutation (MR5) in DivIVA$_{Ef}$ exhibited aberrant cell morphology, such as enlargement, irregular shape and aggregation, indicating interruption of normal cell division. Noticeably, the abolition of the N-terminal coiled-coil disrupted its apparent biological function even though self-interaction/oligomerization was retained. The functional deficits of the N-terminal mutation in *E. faecalis* MWMR5 may be attributed to the disruption of interactions with other cell division proteins in *E. faecalis*. For example, in *B. subtilis*, the N-terminal residues R18 and G19, which are not part of the N-terminal coiled-coil but are conserved across species (black arrows, Supplementary Materials, Fig. A), form a polar targeting determinant (*13*) and play a crucial role in retaining the division inhibitor MinCD (which is not present in *E. faecalis*) at the cell pole after division is complete (*8*). In this process, DivIVA$_{Bs}$ must accumulate at the cell poles by a yet unknown affinity mechanism or through interaction with proteins involved in peptidoglycan biosynthesis (*12*). The A78 amino acid is conserved in DivIVA proteins (Star, Supplementary Materials, Fig. A). It was predicted to be located in the hydrophobic core of the proposed coiled-coil structure in DivIVA$_{Bs}$ (*7*, *13*, *17*) and an A78T mutation did not disrupt the ability of DivIVA$_{Bs}$ to self-interact (*17*). Moreover, *B. subtilis* carrying an A78T allele exhibited a phenotype similar to *divIVA*$_{Bs}$ knockout cells (*2*, *7*, *13*). A *S. pneumoniae* mutant carrying DivIVA$_{Spn}$ A78T displayed a 'chainy' phenotype and the mutated protein localized diffusely, although it was visible at the septum and the cell poles like the wild-type DivIVA$_{Spn}$ (*13*). In *S. pneumoniae*, a A78T mutation in *DivIVA* resulted in lost or significantly reduced ability to interact with divisome proteins such as FtsK, FtsL, FtsQ, FtsB or FtsW although its interaction with itself and with the early divisome proteins (e.g. FtsZ, FtsA, EzrA and ZapA) were retained (*14*). We ascertained that residue A78 is not implicated in the predicted N-terminal coiled-coil in either DivIVA$_{Ef}$, DivIVA$_{Bs}$ or DivIVA$_{Spn}$. The effects of the corresponding A78 mutation on the biological function of DivIVA$_{Ef}$ were not investigated in the present study. Instead, we identified mutations (E37P/N43P/L46D/L50E/L57F) in DivIVA$_{Ef}$ which disrupted the predicted N-terminal coiled-coil structure and which abolished its proper biological function in *E. faecalis*. *S. pneumoniae* and *E. faecalis* are closely related phylogenetically (*4*). Therefore, our results provide further evidence for the important role of the conserved DivIVA N-terminus for the proper biological function of this protein.

E. faecalis MR10 (*i.e.* L143P mutation in *divIVA*$_{Ef}$ predicted to disrupt the second coiled-coil in the central region) exhibited aberrant phenotypes such as 'spherical' shapes, formation of short chains and asymmetrical division. This mutant strain also lost its ability to self

interact and to form oligomer complexes. This indicated that the central coiled-coil structures are important for both $DivIVA_{Ef}$ oligomerization and biological function. The relationship between DivIVA oligomerization and its biological function has previously been studied in *B. subtilis divIVA* (*7*, *17*). A central region L120P mutation in $divIVA_{Bs}$, corresponding to our $divIVA_{Ef}$ L143P mutation (MR10), produced longer *B. subtilis* cells and easily detectable mini-cells and reduced the size of the $DivIVA_{Bs}$ oligomer complex by 50% (*17*, *19*).

Overexpression of $DivIVA_{Ef}$ induced morphological alterations in *E. coli* cells (*4*). Wild-type $DivIVA_{Ef}$ expression in round *E. coli* KJB24 cells induced aberrant morphology, including cell enlargement, suggesting that this strain is useful as an indicator for functionality of cell division proteins from Gram-positive cocci (*4*). Unlike wild-type $DivIVA_{Ef}$, $DivIVA_{Ef}$ mutations MR10 and MR15 were not able to induce morphological changes in *E. coli* KJB24, suggesting that the central coiled-coil structures and oligomerization of $DivIVA_{Ef}$ are crucial for causing these phenotypic effects. This is supported by expression of mutated $DivIVA_{Ef}$ proteins in rod-shaped *E. coli* PB103 cells. Wild-type $DivIVA_{Ef}$ or $DivIVA_{Ef}$ MR5 mutations caused elongation of *E. coli* PB103, while $DivIVA_{Ef}$ MR10 or MR15 mutations failed to exhibit such changes. Interestingly, overexpression of $DivIVA_{Ef}$ MR5 exhibited the same phenotype as wild-type $DivIVA_{Ef}$ in *E. coli* backgrounds, while it lost its ability to maintain proper cell division when expressed in *E. faecalis*. This may be caused by differences of $DivIVA_{Ef}$ MR5 in interacting with the cell division apparatus in Min-free (*E. faecalis*) or MinCDE-containing (*E. coli*) hosts.

We noted that $DivIVA_{Ef}$ can induce morphological changes in *E. coli* cells. In contrast, GFP-fused $DivIVA_{Bs}$ did not produce filamentous or minicell phenotype in *E. coli* although this fusion recognized and targeted to division sites and cell poles in *E. coli* (*2*). These differences might reflect differences in the protein composition between the two proteins. $DivIVA_{Ef}$ has two coiled-coil structures in the central region, while $DivIVA_{Bs}$ only contains one. $DivIVA_{Ef}$ comprises a longer C-terminus which forms an α-helical structure as compared to $DivIVA_{Bs}$. Further research on which proteins interact with DivIVA in *E. coli* may further explain why these different DivIVA proteins exhibit interesting functional differences in *E. coli* backgrounds.

In summary, our research demonstrates that $DivIVA_{Ef}$ forms an oligomer *in vitro* comprising 10–12 monomers. The central region, containing two predicted coiled-coil structures, but not the predicted N-terminal or C-terminal coiled-coils, is responsible for complex formation in this protein. Mutations aimed at the disruption of the central coiled-coil structures altered the biological functioning of $DivIVA_{Ef}$ in both *E. faecalis* and *E. coli* backgrounds. Interestingly, disruption of the N-terminal coiled-coil disrupted cell division functions in *E. faecalis*, but not *E. coli*. This study is the first to provide data on the role of $DivIVA_{Ef}$ coiled-coil structures in oligomer formation and biological function.

Supplementary data are available at *JB* Online.

This project was supported by the Hospital for Sick Children Foundation (Grant# XG 02-075R to J.R.D.) and the Natural Science & Engineering Research Council of Canada (Grant# RGPIN-203651-2006 to J.R.D.). We thank N. F. Eng (U of Ottawa) and K. Bell (U of Saskatchewan) for their technical assistance or advice. Transmission electron microscopy was conducted at the Electron Microscopy Unit, Surgical Medical Research Institute, University of Alberta (Edmonton, Alberta) by M. Chen. We are grateful to P. Anderson (University of Ottawa) for the use of size exclusion chromatography equipment.

REFERENCES

1. Edwards, D.H. and Errington, J. (1997) The *Bacillus subtilis* DivIVA protein targets to the division septum and controls the site specificity of cell division. Mol. Microbiol. **24**, 905–915
2. Edwards, D.H., Thomaides, H.B., and Errington, J. (2000) Promiscuous targeting of *Bacillus subtilis* division protein DivIVA to division sites in *Escherichia coli* and fission yeast. EMBO J. **19**, 2719–2727
3. Vicente, M. and Garcia-Ovalle, M. (2007) Making a point: the role of DivIVA in streptococcal polar anatomy. J. Bacteriol. **189**, 1185–1188
4. Ramirez-Arcos, S., Liao, M., Marthaler, S., Rigden, M., and Dillon, J.R. (2005) *Enterococcus faecalis divIVA*: an Essential gene involved in cell division, cell growth, and chromosome segregation. Microbiol. **151**, 1381–1393
5. Akiyama, T., Inouye, S., and Komano, T. (2003) Novel developmental genes, *fruCD*, of *Myxococcus xanthus*: involvement of a cell division protein in multicellular development. J. Bacteriol. **185**, 3317–3324
6. Marston, A.L., Thomaides, H.B., Edwards, D.H., Sharpe, M.E., and Errington, J. (1998) Polar localization of the MinD protein of *Bacillus subtilis* and its role in selection of the mid-cell division site. Genes Dev. **12**, 3419–3430
7. Cha, J.H. and Stewart, G.C. (1997) The divIVA minicell locus of *Bacillus subtilis*. J. Bacteriol. **179**, 1671–1683
8. Marston, A.L. and Errington, J. (1999) Selection of the midcell division site in *Bacillus subtilis* through MinD-dependent polar localization and activation of MinC. Mol. Microbiol. **33**, 84–96
9. Wu, L.J. and Errington, J. (2003) RacA and the Soj-Spo0J system combine to effect polar chromosome segregation in sporulaing *Bacillus subtilis*. Mol. Microbiol. **49**, 1463–1475
10. Fadda, D., Pischedda, C., Caldara, F., Whalen, M.B., Anderluzzi, D., Domenici, E., and Massidda, O. (2003) Characterization of *divIVA* and other genes located in the chromosomal region downstream of the *dcw* cluster in *Streptococcus pneumoniae*. J. Bacteriol. **185**, 6209–6214
11. Ramos, A., Honrubia, M.P., Valbuena, N., Vaquera, J., Mateos, L.M. and Gil, J.A. (2003) Involvement of DivIVA in the morphology of the rod-shaped actinomcete *Brevibacterium lactofermentum*. Microbiol. **149**, 3531–3542
12. Flardh, K. (2003) Essential role of DivIVA in polar growth and morphogenesis in Streptomyces coelicolor A3(2). Mol. Microbiol. **49**, 1523–1536
13. Perry, S.E. and Edwards, D.H. (2004) Identification of a polar targeting determinant for *Bacillus subtilis* DivIVA. Mol. Microbiol. **54**, 1237–1249
14. Fadda, D., Santona, A., D'Ulisse, V., Ghelardini, P., Ennas, M.G., Whalen, M.B., and Massidda, O. (2007) *Streptococcus pneumoniae* DivIVA: localization and interactions in a MinCD-free context. J. Bacteriol. **189**, 1288–1298
15. Massidda, O., Anderluzzi, D., Friedli, L., and Feger, G. (1998) Unconventional organization of the division and cell wall gene cluster of *Streptococcus pneumoniae*. Microbiol. **144**, 3069–3078

16. Pinho, M.G. and Errington, J. (2004) A divIVA null mutant of *Staphylococcus aureus* undergoes normal cell division. FEMS Microbiol. **240**, 145–149
17. Muchova, K., Kutejova, E., Scott, D.J., Brannigan, J.A., Lewis, R.J., Wilkinson, A.J., and Barak, I.A. (2002) Oligomerization of the *Bacillus subtilis* division protein DivIVA. Microbiol. **148**, 807–813
18. Muchova, K., Kutejova, E. Pribisova, L., Wilkinson, A.J., and Barak, I. (2002) *Bacillus subtilis* division protein DivIVA - screen for stable oligomer state conditions. Acta Crystallogr. D. Biol. Crystallogr. **58**, 1542–1543
19. Stahlberg, H., Kutejova, E., Muchova, K., Gregorini, M., Lustig, A., Muller, S.A., Olivieri, V., Engel, A., Wilkinson, A.J., and Barak, I. (2004) Oligomeric structure of the *Bacillus subtilis* cell division protein DivIVA determined by transmission electron microscopy. Mol. Microbiol. **52**, 1281–1290
20. Miroux, B. and Walker, J.E. (1996) Over-production of proteins in *Escherichia coli*: mutant hosts that allow synthesis of some membrane proteins and globular proteins at high levels. J. Mol. Biol. **260**, 289–298
21. de Boer, P.A., Crossley, R.E., and Rothfield, L.L. (1988) Isolation and properties of *minB*, a complex genetic locus involved in correct placement of the division site in *Escherichia coli*. J. Bacteriol. **170**, 2106–2112
22. Begg, K.J. and Donachie, W.D. (1998) Division planes alternate in spherical cells of *Escherichia coli*. J. Bacteriol. **180**, 2564–2567
23. Jacob, A.E. and Hobbs, S.J. (1974) Conjugal transfer of plasmid-borne multiple antibiotic resistance in *Streptococcus faecalis* var. zymogenes. J. Bacteriol. **117**, 360–372
24. Szeto, J., Eng, N.F., Acharya, S., Rigden, M.D., and Dillon, J.A. (2005) A conserved polar region in the cell division site determinant MinD is required for responding to MinE-induced oscillation but not for localization within coiled arrays. Res. Microbiol. **156**, 17–29
25. Sambrook, J. F. E. F. a. M. T. (1980) *Molecular Cloning: A Laboratory Manual,* Cold Spring Harbor Press, New York
26. Amersham Biosciences. (2002) *Gel Filtration: Principles and Methods*, Amersham Biosciences. GE Healthcare Bio-Science AB, Björkgatan 30, 751–84 Uppsala, Sweden.
27. Szeto, J., Acharya, S., Eng, N.F., Dillon, , and Jo-Anne, (2004) The N terminus of MinD contains determinants which affect its dynamic localization and enzymatic activity. J. Bacterol. **186**, 7175–7185
28. Poyart, C. and Trieu-Cuot, P. (1997) A broad-host-range mobilizable shuttle vector for the construction of transcriptional fusions to beta-galactosidase in gram-positive bacteria. FEMS Microbiol. Lett. **156**, 193–198
29. Callegan, M.C., Jett, B.D., Hancock, L.E., and Gilmore, M.S. (1999) Role of hemolysin BL in the pathogenesis of extraintestinal *Bacillus cereus* infection assessed in an endophthalmitis model. Infect. Immun. **67**, 3357–3366
30. Bryan, E.M., Bae, T., Kleerebezem, M., and Dunny, G.M. (2000) Improved vectors for nisin-controlled expression in gram-positive bacteria. Plasmid **44**, 183–190
31. Lupas, A. (1996) Prediction and analysis of coiled-coil structures. Methods Enzymol. **266**, 513–525
32. Lupas, A., Van Dyke, M., and Stock, J. (1991) Predicting coiled coils from protein sequences. Science **252**, 1162–1164
33. Query, C.C., Bentley, R.C., and Keene, J.D. (1989) A common RNA recognition motif identified within a defined U1 RNA binding domain of the 70K U1 snRNP protein. Cell **57**, 89–101
34. Armstrong, D.J. and Roman, A. (1993) The anomalous electrophoretic behavior of the human papillomavirus type 16 E7 protein is due to the high content of acidic amino acid residues. Biochem. Biophys. Res. Commun. **192**, 1380–1387
35. Hu, C.C. and Ghabrial, S.A. (1995) The conserved, hydrophilic and arginine-rich N-terminal domain of cucumovirus coat proteins contributes to their anomalous electrophoretic mobilities in sodium dodecylsulfate-polyacrylamide gels. J. Virol. Methods **55**, 367–379
36. Iakoucheva, L.M., Kimzey, A.L., Masselon, C.D., Smith, R.D., Dunker, A.K., and Ackerman, E.J. (2001) Aberrant mobility phenomena of the DNA repair protein XPA. Protein Sci. **10**, 1353–1362
37. Cozzone, A.J., Grangeasse, C., Doublet, P., and Duclos, B. (2004) Protein phosphorylation on tyrosine in bacteria. Arch. Microbiol. **181**, 171–181
38. Kang, C.-M., Abbott, D.W., Park, S.T., Dascher, C.C., Cantley, L.C., and Husson, R.N. (2005) The *Mycobacterium tuberculosis* serine/threonine kinases PknA and PknB: substrate identification and regulation of cell shape. Genes Dev. **19**, 1692–1704